Stresses and Crack Tip Stress Intensity Factors Around Spherical and Cylindrical Voids and Inclusions of Differing Elastic Properties and with Misfit Sizes

Paul C. Paris, Thierry Palin-Luc, Hiroshi Tada and Nicolas Saintier

Arts et Metiers Paris Tech, Université Bordeaux 1, LAMEFIP, Esplanade des Arts et Metiers, F33405 Talence Cedex, France

ABSTRACT. *In gigacycle fatigue, crack initiation and growth most often occurs from internal defects in the material including holes and inclusions. Occasionally a surface defect of hemi-spherical shape is also encountered. In order to attempt to understand the stresses near these imperfections and the stress intensity factors for cracks initiating from them, some elastic stress formulae will be developed here. For the inclusions mismatches in elastic properties and sizes will be treated for realistic examination of their effects. It is hoped that convenient availability of such formulae may enhance an understanding of gigacycle fatigue initiation and crack growth.*

SPHERICAL CAVITIES AND INCLUSIONS

Under uni-axial stress, σ, the *spherical cavity* will have a stress concentration factor, K_t, which is defined by:

$$\sigma_{\max} = K_t \sigma \tag{1}$$

The concentration factor for this case is given in standard texts on Theory of Elasticity [1] as:

$$K_t = \frac{3}{2}\left(1+\frac{2}{7-5\nu}\right) \qquad \text{(where } \nu \text{ is Poisson's ratio)} \tag{2}$$

On the other hand *for tri-axial tension,* $\overline{\sigma}$, the stress concentration factor is simply:

$$K_t = 3/2 \tag{3}$$

Moreover, if instead of an internal spherical cavity, the *hemispherical surface cavity* is the case of interest, the increase in the stress concentration factor is less that 2% for the uni-axial case or:

$$K_t = 1.522\left(1+\frac{2}{7-5\nu}\right) \tag{4}$$

The stress outside the *spherical cavity under uni-axial loading* is given at a radial distance, r, compared to the radius of the sphere, *R*, by:

$$\sigma_{axial} = \left[1+\frac{4-5\nu}{14-10\nu}\frac{R^3}{r^3}+\frac{9}{14-10\nu}\frac{R^5}{r^5}\right]\sigma \tag{5}$$

Further for the *spherical cavity under tri-axial loading, $\overline{\sigma}$, with internal pressure, p,* the result in spherical coordinates is:

$$\sigma_\theta = \sigma_\varphi = \overline{\sigma} + \frac{(\overline{\sigma}+p)R^3}{2r^3} \text{ and } \sigma_r = \overline{\sigma} - \frac{(\overline{\sigma}+p)R^3}{2r^3} \text{ for } r \geq R \tag{6}$$

Both of these formulae give the stresses on a prospective crack plane extending outward from the cavity. For the latter case in Eq. (6) the radial displacement from the surface of the cavity outward is given Eq. (7) where *E* is the elastic modulus.

$$u_{r-cavity} = \frac{(1+\nu)(\overline{\sigma}+p)}{2E}\frac{R^3}{r^2} + \frac{(1-2\nu)\overline{\sigma}r}{E} \tag{7}$$

For the spherical inclusion with external pressure, *p*, the radial displacement of the surface is:

$$u_{r-inclusion} = -\frac{(1-2\nu')pR}{E'} \tag{8}$$

where E' and ν' are the elastic constants of the inclusion.

If the spherical inclusion is larger than the spherical cavity it occupies, then there will be a contact pressure, p, which will also depend on the external hydrostatic tension, $\overline{\sigma}$. The mismatch shall be that of an inclusion which is larger by a radial amount, Δ. Then the compatibility of the radial displacements between the cavity and inclusion can be expressed as:

$$u_{r-inclusion} + \Delta = u_{r-cavity} \qquad (\text{at } r = R) \tag{9}$$

Combining Eqs. (7, 8 and 9) leads to an additional stress outside the cavity as:

$$\sigma_\theta(r=R) = \left(\frac{\Delta}{2R}\right) \Bigg/ \left(\frac{1+\nu}{2E} + \frac{1-2\nu'}{E'}\right) \tag{10}$$

which should be added to the previous stress result Eq. (6) with $r = R$ and *p=0*. Under such circumstances the pressure, *p*, generated between the inclusion and the matrix is given Eq. (11). The contact between inclusion and matrix is lost if $\Delta / R \leq 3(1-\nu)\overline{\sigma}/(2E)$.

$$p = \left[\frac{\Delta}{R} - \frac{3}{2}\frac{(1-\nu)}{E}\overline{\sigma}\right] \Bigg/ \left[\frac{1+\nu}{2E} + \frac{(1-2\nu')}{E'}\right] \qquad \text{(compression)} \tag{11}$$

Now, if there is no mismatch and the inclusion is bonded to the external body, then the stress concentration is:

$$K_t = \frac{3}{2}\left\{1 - \left[\frac{1-\nu}{2E}\right] \Bigg/ \left[\frac{1-2\nu'}{E'} + \frac{1+\nu}{2E}\right]\right\} \tag{12}$$

Notice that for $E' = 0$ that $K_t = 3/2$; for $E' = E, \nu' = \nu$ that $K_t = 1$;
and for $E' = \infty$ that $K_t = \frac{3\nu}{1+\nu}$ which is as expected. With this in mind the stress in the body next to the inclusion is:

$$\sigma_{\theta-\max}(r = R^+) = K_t\overline{\sigma} + \left(\frac{\Delta}{2R}\right) \Bigg/ \left(\frac{1+\nu}{2E} + \frac{1-2\nu'}{E'}\right) \tag{13}$$

This form accommodates a bonded inclusion of differing elastic properties and with a mismatch in its size compared to the void in the main body. As a first approximation it is suggested here for the case of uni-axial stress applied to the body that the K_t be increased by the ( ) factor in Eq.(2).

CYLINDRICAL CAVITIES AND INCLUSIONS

For cylindrical cavities and inclusions the case may be plane stress or plane strain depending on constraint conditions. For that reason it is convenient to use modified elastic constants, *G*, the shear modulus, and β which depends on the Poisson's ratio but changes with the constraint. They are defined as:

$G = \dfrac{E}{2(1+\nu)}$ and $\beta = 1-\nu$ for plane strain and $\beta = \dfrac{1}{1+\nu}$ for plane stress. For the inclusion they shall be written with a prime. For plane stress it is assumed that the cylindrical void and the cylindrical inclusion are smooth (frictionless) and unbounded. For both constraint cases the biaxial (or tri-axial) exterior applied stress is taken as $\overline{\sigma}$, and the contact pressure between the void and cylinder is *p*.

The classical equations for the stresses in the outer body are:

$$\sigma_r(r \geq R) = \overline{\sigma} - \frac{(p+\overline{\sigma})R^2}{r^2} \tag{14}$$

and $$\sigma_\theta(r \geq R) = \overline{\sigma} + \frac{(p+\overline{\sigma})R^2}{r^2} \tag{15}$$

which lead to the radial displacement given by:

$$2Gu_r(r \geq R) = (2\beta - 1)\overline{\sigma} r + \frac{(p+\overline{\sigma})R^2}{r} \tag{16}$$

The compatibility of displacements between the void and inclusion is the same as previously for the inclusion of larger radius by Δ than the void, the result is:

$$u_{r-inclusion}(r = R) + \Delta = u_{r-void}(r = R) \tag{17}$$

which leads to the pressure between inclusion and matrix:

$$p = 2\left[\frac{\Delta}{R} - \frac{\beta\overline{\sigma}}{G}\right] \bigg/ \left[\frac{1}{G} + \frac{2\beta' - 1}{G'}\right] \tag{18}$$

This can be used to get the maximum stress in the body, Eq. (19) as long as contact is not lost, $p \geq 0$.

$$\sigma_{\theta-\max}(r = R^+) = p + 2\overline{\sigma} \tag{19}$$

Further, the stress concentration factor in Eq. (19) of 2 can be changed to 3 for uni-axial exterior applied stresses, $\overline{\sigma}$, as a first approximation for that case of stressing.

Finite element analysis

Finite element computations have been performed in order to validate the proposed analytical solutions. All loading cases presented above have been computed: axisymetrical pressure and axial loading, plane stress and plane strain pressure and axial loading. In all cases we consider an inclusion and a matrix of differing elastic properties; and with a mismatch in the inclusion size compared to the void in the matrix. The elastic properties and mismatch values have been chosen so that reasonable maximum stress (around 100 MPa) was obtained in the matrix and in the inclusion when the external loading was zero (stress induced by the mismatch only). The following values were chosen: E=220GPa, ν =0.3, E'=440GPa, ν=0.28 and Δ / R =0.001.

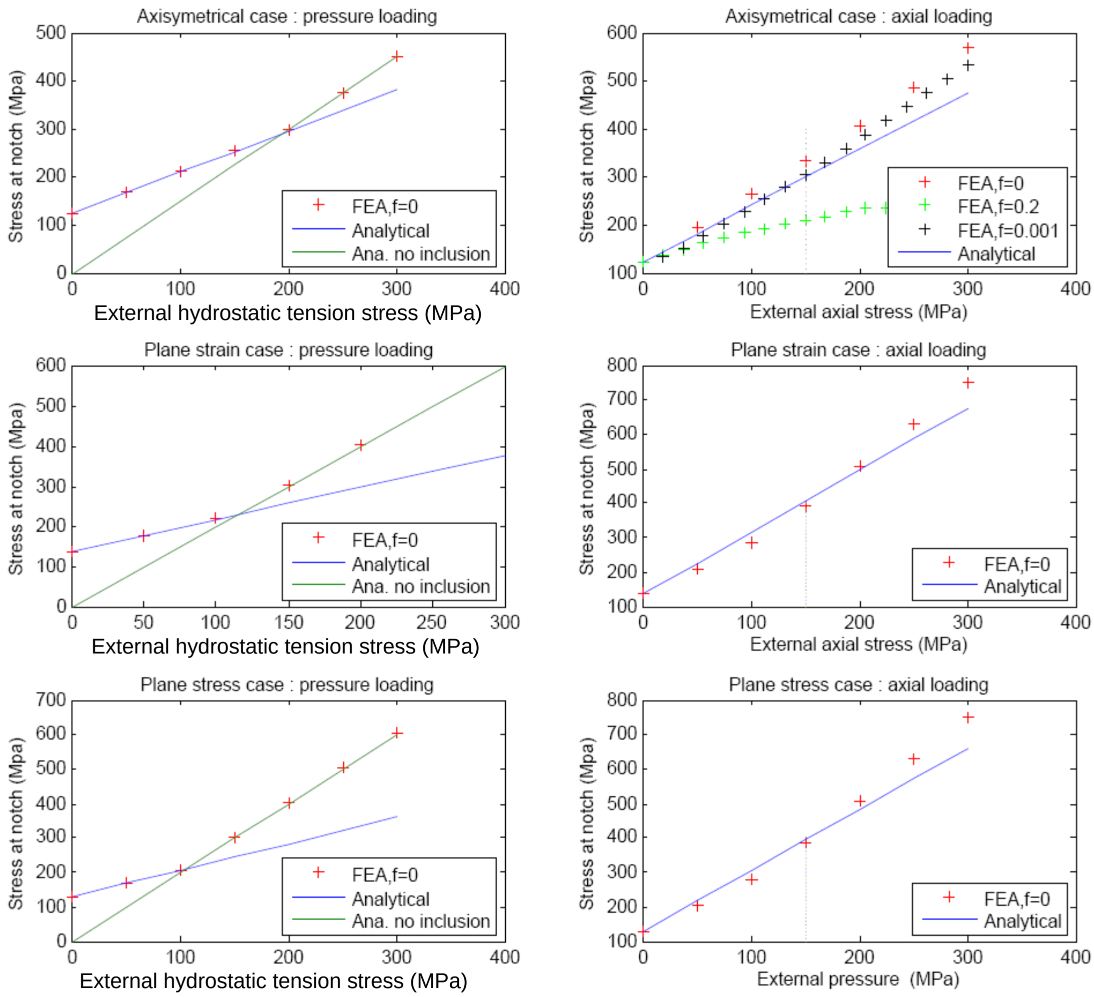

Figure 1. Comparison between analytical and FEA resu[illegible]ersus external hydrostatic tension stress $\bar{\sigma}$.

All the results are presented figure 1. For each loading case the analytical and FE result are compared. For the pressure loading cases (left part of the figure) analytical and FEA results show a perfect match independently of the stress state. The reason why two different slopes are observed is the following. For low external loading inclusion and matrix are in contact; the FEA results match the analytical solution that take into account the inclusion. However, once the external loading reaches a critical value the contact is lost due to the matrix deformation. For pressure values above this critical pressure the FEA solution matches the analytical solution corresponding to a void in an infinite matrix as expected (second slope).

For the axial loading case (right part of figure 1) FEA and analytical results show reasonably good match but less than in the pressure case. It has to be noticed that the global to local stress/external stress is not linear anymore. The reason is that in this case, the contact lost in between the inclusion and the matrix is not a linear function of the external load so that the global to local stress response can not be linear either.

STRESS INTENSITY FACTORS AT CRACK TIPS GROWING FROM VOIDS AND INCLUSIONS SOME WITH MISMATCHED SIZES

In order to give estimates of the crack tip stress intensity factors for cracks starting at the voids or inclusions and growing to failure, asymptotic approximation methods will be adopted. It consists of exactly fitting the exact stress intensities for small racks sizes and also for large crack sizes and then fitting a smooth cubic curve between these exact solutions. As a first example the results of such a method are presented for a hemispherical void on the surface of a solid, such as might occur due to a corrosion pit.

Cracking from a hemispherical surface void with a spherical radius R and a crack of depth a measured from the surface of the hemisphere, the asymptotic approximation of the crack tip stress intensity factor is (making use of the 1.015 factor for the half plane effect): $K = 1.015\sigma\sqrt{\pi a} \cdot F(x,\nu)$ where $x = \frac{a}{R}$ for $0 \le \frac{a}{R} \le \infty$ (20)

where $F(x,\nu) = A(\nu) + B(\nu)\frac{x}{1+x} + C(\nu)\left(\frac{x}{1+x}\right)^2 + D(\nu)\left(\frac{x}{1+x}\right)^3$ (21)

Further the coefficients A, B, C and D are found to be: $A(\nu) = 1.683 + \frac{3.366}{7-5\nu}$

$B(\nu) = -1.025 - \frac{12.3}{7-5\nu}$, $C(\nu) = -1.089 + \frac{14.5}{7-5\nu}$, $D(\nu) = 1.068 - \frac{5.568}{7-5\nu}$ (22)

These coefficients are for both uniaxial stress or biaxial stress, σ, applied parallel to the surface from which the pit emanates. However, the 1.015 factor in Eq. (20) is for the deepest part of the crack front away from the surface forming the hemisphere.
With an angle θ measured from a line perpendicular to that surface, the factor, 1.015, may be replaced by: $f(\theta) = 1.210 - 0.195\sqrt{\cos\theta}$ for $(-80° \le \theta \le 80°)$ (23)
in order to get the stress intensity factor, *K*, along the crack front. Adjustments may be made in these values for *K* due to the imperfection in the hemispherical shape or unequal depth of the crack, *a*, around the hemisphere as suggested in Appendix I of the "Stress Analysis of Cracks Handbook" by Tada, Paris, and Irwin [2].

For the stress intensity factor for a crack growing from a mismatched in size spherical inclusion or void the analysis follows. The crack size, *a*, measured from the surface of

the spherical inclusion into the surrounding body shall be represented here by, $\bar{a}$, measured from the center of the inclusion or void. This is expressed by: $\bar{a} = R + a$, where R is the radius of the sphere. This assumes no difference in material properties.
For *very large cracks* ringing the sphere, $\bar{a}/R >> 1$, the mismatched spherical inclusion is larger by imposing, Δ, as the size of the mismatch. For a large ring crack the load, *P*, imposed on the exterior body is:

$$P = 2ER\Delta/(1-\nu^2) \tag{24}$$

The stress intensity factor for the opposing concentrated loads, *P*, in the center of a circular crack is:

$$K_\Delta = \frac{P}{(\pi\bar{a})^{3/2}} = \frac{2ER\Delta}{(1-\nu^2)(\pi\bar{a})^{3/2}} \tag{25}$$

The additional stress intensity factor due to uniform normal stress, σ perpendicular to the crack (any additional normal stresses parallel to the crack have no effect) is:

$$K_\sigma = \frac{2}{\pi}\sigma\sqrt{\pi\bar{a}}\left(1 - \frac{4R}{\pi^2\bar{a}}\right) \tag{26}$$

where the sum of these give the total stress intensity factor for large cracks:

$$K_{total} = K_\Delta + K_\sigma \tag{27}$$

On the other hand *for small cracks* emanating into the surrounding body from the inclusion, $\bar{a}/R = (R+a)/R \cong 1^+$ the results are:

$$K_\Delta = E\Delta\Big/\left[2(1-\nu^2)\sqrt{\pi\left(\frac{\bar{a}-R}{2}\right)}\right] \qquad K_\sigma = \sigma\sqrt{\pi\frac{(\bar{a}-R)}{2}} \qquad K_{total} = K_\Delta + K_\sigma \tag{28}$$

From the first expression in Eq. (28) and Eq. (25) the final asymptotic approximation is:

$$K_\Delta = \frac{E\Delta}{(1-\nu^2)\pi\sqrt{\pi\bar{a}}}\left(\frac{R}{\bar{a}}\Big/\sqrt{1-\frac{R}{\bar{a}}}\right)F_\Delta\left(\frac{R}{\bar{a}}\right) \tag{29}$$

where: $F_\Delta(R/\bar{a}) = 1 - 0.5(R/\bar{a}) + 2.44(R/\bar{a})^2 - 1.83(R/\bar{a})^3$ (30)

Further for the asymptotic relationship for σ the result is:

$$K_\sigma = \sigma\sqrt{\pi\bar{a}}\left(\sqrt{\left(1-\frac{R}{\bar{a}}\right)\Big/2}\right)F_\sigma\left(\frac{R}{\bar{a}}\right) \tag{31}$$

where: $F_\sigma(R/\bar{a}) = 0.900 + 0.085(R/\bar{a}) + 0.015(R/\bar{a})^2$ (32)

And again the final approximation for $1 \le \frac{\bar{a}}{R} \le \infty$ combines Eqs. (29) through (32) with:

$$K_{total} = K_\Delta + K_\sigma \tag{33}$$

Now, consider crack tip stress intensity factors for *cylindrical inclusions with mismatch in both size and material elastic properties*. For small cracks into the exterior body of length, *a*, as compared to the radius, *R*, of the cylindrical inclusion, or $a/R << 1$, the stresses at the initial crack site, σ_0, and its reduction at the crack tip, σ_1, as caused by the gradient away from the inclusion are:

$$\sigma_0 = \sigma_\theta(r = R) = 2\overline{\sigma} + p \tag{34}$$

where as before $\overline{\sigma}$ is the externally applied biaxial stress and p is the contact pressure. Then: $\sigma_1 = \dfrac{d\sigma_\theta(r = R)}{dr} a = 2\overline{\sigma}\left(1 - 2\beta\dfrac{G_{eff}}{G}\right)\dfrac{a}{R}$ (35)

where $1/G_{eff} = 1/G + (2\beta' - 1)/G'$ (36)

Now, *for the case of no misfit between the inclusion and exterior body,* and bonded together for plane strain or smooth frictionless contact for plane stress between them, the stress intensity factor is of the form:

$$K_\sigma = \overline{\sigma}\sqrt{\pi a}F_\sigma(a/R, \gamma, G_{eff}/G) \tag{37}$$

where F_σ is defined by Eq. (38) and where $\gamma = G'/G$ which applies for $a/R << 1$.

$$F_\sigma\left(\frac{a}{R}, \gamma, \frac{G_{eff}}{G}\right) = 2\left[\left(1 + 0.122\frac{1}{1+\gamma}\right)\left(1 - \beta\frac{G_{eff}}{G}\right) - \frac{2}{\pi}\left(1 + 0.073\frac{1}{1+\gamma}\right)\left(1 - 2\beta\frac{G_{eff}}{G}\right)\frac{a}{R}\right] \tag{38}$$

Now, *for large cracks* the values of F_σ approach asymptotically to constants which are:

$F_\sigma(\ ) = 1$ (for cracks on both sides of the inclusion)

$F_\sigma(\ ) = 1/\sqrt{2}$ (for a crack on one side of the inclusion)

Further for the full range of crack sizes $0 < a/R < \infty$ the cubic asymptotic fit of the end curves will be applied. It is: $F_\sigma(x, \gamma, \gamma_{eff}) = A + B\left(\dfrac{x}{1+x}\right) + C\left(\dfrac{x}{1+x}\right)^2 + D\left(\dfrac{x}{1+x}\right)^3$ (39)

where: $A(\gamma, \gamma_{eff}) = 2(1 + 0.122/(1+\gamma))(1 - \beta\gamma_{eff})$

$$B(\gamma, \gamma_{eff}) = -\frac{\pi}{4}(1 + 0.073/(1+\gamma))(1 - 2\beta\gamma_{eff}) \tag{40}$$

For *cracks on both sides* of the incusion:

$$C(\gamma, \gamma_{eff}) = 3 - 3A - 2B \quad , \quad D(\gamma, \gamma_{eff}) = -2 + 2A + B \tag{41}$$

where: $x = a/R$, $\gamma = G'/G$, $\gamma_{eff} = G_{eff}/G$

However, *for a crack on one side of the inclusion* Eqs. (41) should be replaced by Eqs. (42). This completes the discussion for the externally applied stresses with differing elastic properties of the inclusion.

$$C = 2.121 - 3A - 2B \quad , \quad D = -2 + 2A + B \tag{42}$$

Next the case of a radial difference, Δ, interference between the inclusion and its nest in the exterior body will be considered. For small cracks $a/R << 1$ on one side or both sides of the inclusion the result is:

$$K_\Delta = 2G_{eff}\frac{\Delta}{R}\sqrt{\pi a}F_\Delta\left(\frac{a}{R}, \gamma\right) \tag{43}$$

where: $F_\Delta(a/R, \gamma) = 1 + 0.122/(1+\gamma) - \dfrac{4}{\pi}(1 + 0.073/(1+\gamma))\, a/R$ (44)

For large cracks, $a/R >> 1$, the result for a crack on *one side of the inclusion* is:

$$K_{\Delta} = \frac{G_{eff}\Delta}{\beta\sqrt{\pi a}}\sqrt{1\Big/\left[\frac{a}{R}\left(2+\frac{a}{R}\right)\right]} \qquad (45)$$

The asymptotic interpolation between these solutions for large and small cracks on *one side of the inclusion* is:

$$K_{\Delta} = G_{eff}\frac{\Delta}{R}\sqrt{\pi a}F_{\Delta}(x,\gamma) \qquad (46)$$

where: $F_{\Delta}(x,\gamma) = A + B\left(\frac{x}{1+x}\right) + C\left(\frac{x}{1+x}\right)^2 + D\left(\frac{x}{1+x}\right)^3$ (47)

with: $A(\gamma) = 2\pi f_0$, $B(\gamma) = -8 f_1$, $C(\gamma) = -6\pi f_0 + 16 f_1$, $D(\gamma) = 4\pi f_0 - 8 f_1$ (48)

and: $f_0 = 1 + 0.122/(1+\gamma)$, $f_1 = 1 + 0.073/(1+\gamma)$ (49)

Finally, these results, from Eqs. (37) through (49), may be combined to get the total stress intensity factor from: $K_{total} = K_{\sigma} + K_{\Delta}$ (50)

The intended application of this work is to analyze the initiation and growth of cracks in gigacycle fatigue. For that purpose Eq. (50) putting in the maximum stress, σ , to get the maximum stress intensity factor. For the range of the stress intensity factor, since the K_{Δ} imposes a constant stress intensity factor, the range should be computed from the K_{σ} only by Eq. (51). But, Eq. (50) shows that the R ratio $K_{total,\min}/K_{total,\max}$ is different from $K_{\sigma,\min}/K_{\sigma,\max}$ due to the cyclic loading.

$$\Delta K_{total} = \Delta K_{\sigma} \qquad (51)$$

CONCLUSION

The local elastic stresses and the theoretical stress concentration factors near inclusions mismatches in elastic properties and sizes, and included in a matrix under uniaxial loading or external hydrostatic tension were computed. The stress intensity factors for cracks initiating from them was approximated too by some elastic stress formulas. It is hoped that convenient availability of such formulas may enhance an understanding of gigacycle fatigue initiation and crack growth.

Acknowledgements

The authors acknowledge Arts et Metiers ParisTech and Foundation Arts et Metiers for the financial support of Paul C. Paris' stay at LAMEFIP in 2009. The encouragement of Prof. Ivan Iordanoff, Director of LAMEFIP, is also acknowledged with thanks

REFERENCES

1. Peterson R.E. (1974) Stress concentration factors, Wiley-Interscience, New-York.
2. Tada H., Paris P.C. and Irwin G.R. (2000) *The Stress Analysis of Cracks Handbook*, 3rd edition, ASME Press.